Peptide Folding and Assembly

DOI: 10.1002/anie.201403506

Coordination-Driven Folding and Assembly of a Short Peptide into a Protein-like Two-Nanometer-Sized Channel**

Tomohisa Sawada, Asami Matsumoto, and Makoto Fujita**

Abstract: *Short peptide helices have attracted attention as suitable building blocks for soft functional materials, but they are rarely seen in crystalline materials. A new artificial nanoassembly of short peptide helices in the crystalline state is presented in which peptide helices are arranged three-dimensionally by metal coordination. The folding and assembly processes of a short peptide ligand containing the Gly-Pro-Pro sequence were induced by silver(I) coordination in aqueous alcohol, and gave rise to a single crystal composed of polyproline II helices. Crystallographic studies revealed that this material possesses two types of unique helical nanochannel; the larger channel measures more than 2 nm in diameter. Guest uptake properties were investigated by soaking the crystals in polar solutions of guest molecules; anions, organic chiral molecules, and bio-oligomers are effectively encapsulated by this peptide-folded porous crystal, with moderate to high chiral recognition for chiral molecules.*

Artificial protein-like functional nanostructures have wide prospects for application in the sophisticated molecular recognition processes and enzymatic reactions of bio-related molecules. In natural systems, polypeptides containing dozens to hundreds of residues are precisely folded into helices, sheets, or turns, and then assembled into well-defined three-dimensional structures. Proteins are often composed of repeated sequences (tandem repeats),[1] and this can be considered an efficient way to produce nanoarchitectures from a limited amount of sequence information. Even in artificial systems, only a small number of peptide residues may ultimately be required for the rational bottom-up synthesis of protein-like architectures through tandem repeats. This idea prompted us to examine the self-assembly of a short peptide fragment using coordination-driven self-assembly, which is a powerful strategy for the construction of well-defined artificial functional nanocavities.[2,3] However, in contrast to conventional rigid ligands, oligopeptides are not easily accessible for such a purpose owing to their conformational flexibility.[4] To overcome this difficulty, we found that, in addition to networking, folding is an essential consideration, as peptide helices are ubiquitously generated in nanostructures.[5] Herein, we describe a new approach for the creation of artificial protein-like nanocavities in which the two key processes, networking and folding, work in concert (Figure 1). The short peptide Gly-Pro-Pro (Gly: glycine, Pro: L-proline), a sequence unit of collagen, was specifically fixed in the polyproline II helix (P_{II} helix) conformation and, at the same time, three-dimensionally networked by coordination-driven self-assembly to afford a single crystalline nanostructure. Although previous examples of crystalline coordination materials with short peptides have been reported, to the best of our knowledge, this is the first report on such a material composed of in situ folded peptide helices.[6,7] Moreover, the helical peptidic conformations and their entanglements generated through metal-coordination provide unique huge nanochannel structures (diameter >2 nm) in the framework, and these were revealed to efficiently take up chiral molecules and bio-related oligomers.

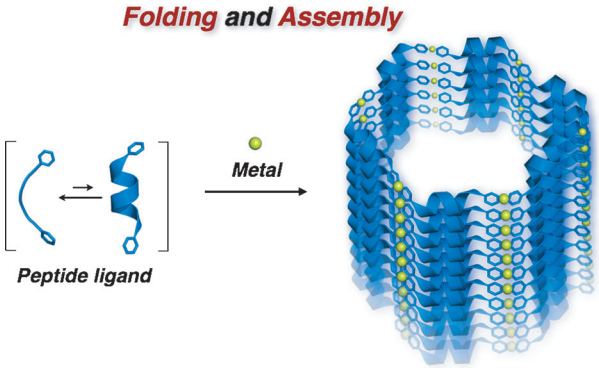

Figure 1. Concept of this work. Random-coil peptide ligands are concomitantly folded through metal-directed networking. Note that the illustration of the network does not represent the network topology of the complex in the present study.

The short peptide Gly-Pro-Pro was modified to generate coordinative ligand **1** by the introduction of 3-pyridyl groups (py) with amide bonds at both termini. Tripeptide ligand **1** was synthesized in two steps of solution-phase peptide synthesis (overall yield: 29%).[8] Ligand **1** showed conformational flexibility in solution: three major conformers were confirmed by ^{1}H NMR measurements (Supporting Information, Figure S3). Circular dichroism measurements also showed that the short fragment of Gly-Pro-Pro was present in a conformationally denatured state in both water and ethanol (Supporting Information, Figure S11). However, when an ethanol solution of **1** (56 mM) was slowly diffused

[*] Dr. T. Sawada, A. Matsumoto, Prof. Dr. M. Fujita
Department of Applied Chemistry, School of Engineering
The University of Tokyo
7-3-1 Hongo, Bunkyo-ku, Tokyo 113-8656 (Japan)
E-mail: tsawada@appchem.t.u-tokyo.ac.jp
mfujita@appchem.t.u-tokyo.ac.jp

[**] This work was supported by Grants-in-Aid for Specially Promoted Research (24000009) and for Young Scientists (B) (25810046).

Supporting information for this article is available on the WWW under http://dx.doi.org/10.1002/anie.201403506.

into an aqueous solution of $AgBF_4$ (56 mM) at 10 °C for one week, colorless block crystals $[(AgBF_4)\cdot\mathbf{1}]_n$ were obtained (Scheme 1, yield: 38 %). Single-crystal X-ray analysis clearly revealed that short peptide ligand **1** is specifically fixed in the P_{II} helix conformation. In the crystalline state, two crystallographically independent ligands **1** are observed (Figure 2a). The dihedral angles ϕ and ψ (ϕ: N-C_α torsion, ψ: C_α-C′ torsion) of the six peptide bonds range from −66 to −108° for

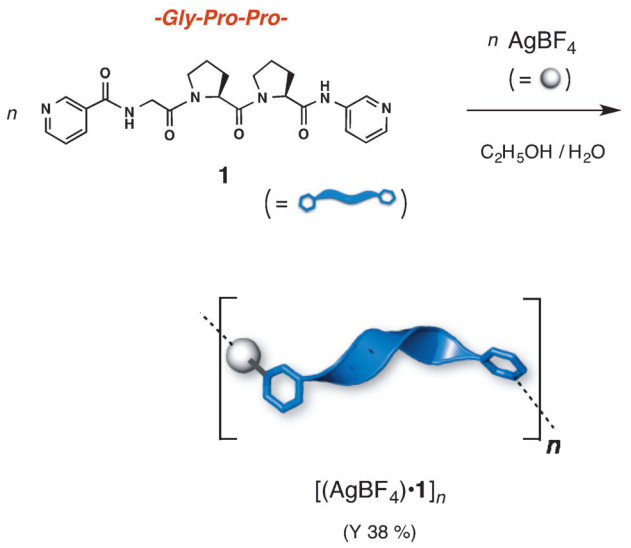

Scheme 1. The crystallization of Gly-Pro-Pro ligand with $AgBF_4$.

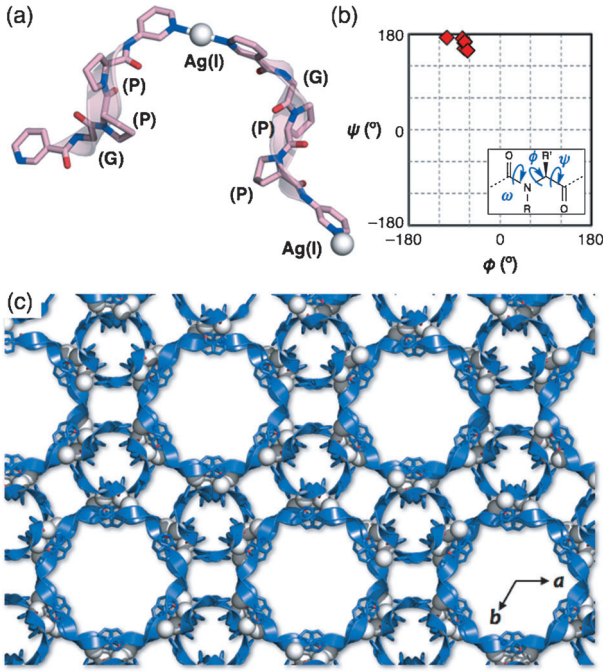

Figure 2. a) Asymmetric unit of the single-crystal X-ray structure of $[(AgBF_4)\cdot\mathbf{1}]_n$. b) Ramachandran plot. c) Networked structure of $[(AgBF_4)\cdot\mathbf{1}]_n$ in the crystalline state. Py groups are represented as blue sticks, peptide helices as blue ribbons, and silver(I) ions as white spheres. Graphics were generated with PyMOL. Solvents, BF_4^- anions, and hydrogen atoms have been omitted for clarity.

ϕ and 150 to 172° for ψ, as shown in the Ramachandran plot (Figure 2b),[9] and all the amide bonds are in the *trans* configuration ($\omega = 180°$). Consequently, the conformation of tripeptide ligand **1** was assigned as the P_{II} helix conformation, for which ϕ, ψ, and ω values are typically −75, 175, and 180°, respectively.

All of the peptide ligands **1** are linked by py-Ag^I-py coordination in a directional N→C-terminal manner, similar to natural polypeptide chains. Furthermore, the linear helical strand of Ag^I-**1** repeats shows a unique hexagonal entanglement in the crystal, which affords a three-dimensional honeycomb network (Figure 2c).[10] Of particular interest is the formation of two types of one-dimensional chiral channel along the crystallographic *c* axis (Figure 3). The larger channel (channel A) is surrounded by ligands **1** in a left-handed duplex-like framework, which is stabilized by π-stacking of the py groups (diameter: 2.2 nm, helical pitch: 2.3 nm). Within this channel A, only surface water solvent molecules could be clearly observed in the X-ray analysis (Supporting Information, Figure S13c). Owing to the very large channel size, the solvents in channel A showed high fluidity and were observed as highly disordered regions of electron density by X-ray diffraction.

In contrast, the smaller channel (channel B) was closely packed with solvents and anions. In particular, two crystallographically independent BF_4^- anions were observed: one firmly trapped at the C-terminal amide of ligand **1** through an N−H···F type hydrogen bond (N···F distance: 2.85 Å) and the other at the C-terminal py group through an C−H···F type hydrogen bond (C···F distance: 3.13 Å) (Supporting Information, Figure S18a).

Despite the close packing, the BF_4^- counterions in the crystalline network were easily exchanged with other anions in a single-crystal-to-single-crystal (SCSC) fashion. For example, anion exchange from BF_4^- to PF_6^- was carried out by soaking the single crystals in a 50 mM solution of $NaPF_6$ in ethanol for 2 d at 10 °C, and the exchange was clearly confirmed by single crystal X-ray analysis (Supporting Information, Figure S18b). Likewise, BF_4^- was exchanged for $CF_3SO_3^-$ in a SCSC fashion (Supporting Information, Figure S18c). Direct crystallization with PF_6^- or $CF_3SO_3^-$ has so far been unsuccessful, and the networks containing these anions can only be formed by anion exchange. These facts explain that the counterion plays an important role in crystallization, although it is easily interchangeable by anion exchange.

Interestingly, a high degree of chiral recognition was observed in larger channel A. After soaking the single crystals of $[(AgBF_4)\cdot\mathbf{1}]_n$ in an ethanol solution of a racemic compound, 1,1′-bi-2-naphthol (**2**, 10 mM), for two weeks at 10 °C, encapsulation of **2** in the crystals was observed. After decomposition of the crystal with aqueous NaCl and extraction with $CDCl_3$, NMR analysis revealed the inclusion of approximately two molecules of **2** per helical pitch of channel A. Chiral-phase HPLC analysis revealed that the *R*-form was favorably encapsulated in the crystal of $[(AgBF_4)\cdot\mathbf{1}]_n$ with 48 % enantiomeric excess (entry 1, Table 1). The opposite enantiomer (*S*)-**2** was also selectively encapsulated in an enantiomeric crystal of $[(AgBF_4)\cdot\mathbf{1}]_n$, which was synthesized

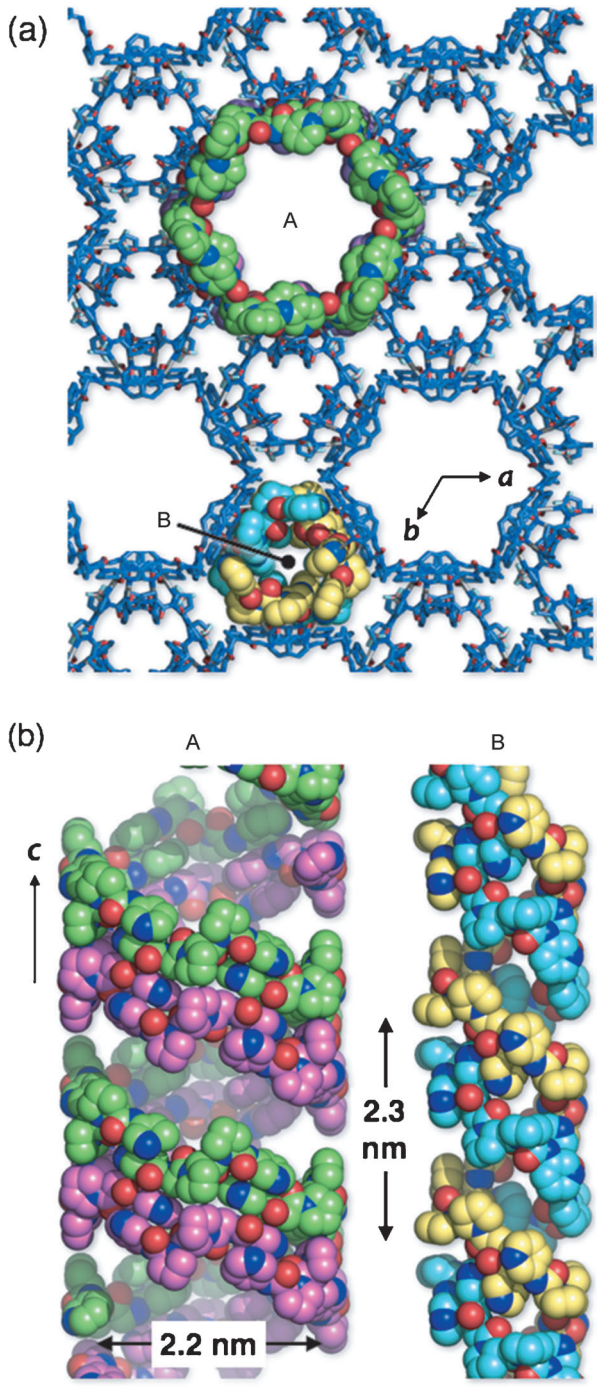

Figure 3. Nanochannel structure in $[(AgBF_4)\cdot\mathbf{1}]_n$. a) Top view: within the whole framework (blue stick representation), larger nanochannel A is highlighted in green/magenta space-filling representation and smaller nanochannel B in cyan/yellow. b) Side view: space-filling representation of nanochannel frameworks A and B. One pseudo-strand (green or magenta) is formed not by chemical bonds but by connection through π-stacking of the py groups. Two such pseudo-strands form a left-handed duplex-like structure (22.8 Å pitch). All solvents and hydrogen atoms have been omitted for clarity.

Table 1: Chiral recognition of **2** by channel A.

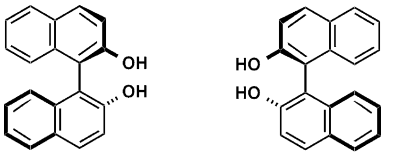

(*R*) (*S*)

2

Entry	*rac*-**2** [mM]	Crystal type[a]	Uptake [molecules/pitch][b]	*S*/*R* ratio[c] (*ee* %)
1	10	L	2.2	26.0/74.0 (*R*, 48)
2	10	D	2.4	74.2/25.8 (*S*, 48)
3	50	L	6.1	32.7/67.3 (*R*, 35)
4	50	D	6.0	67.7/32.3 (*S*, 35)
5	100	L	7.4	36.2/63.8 (*R*, 28)
6	100	D	7.4	63.3/36.7 (*S*, 27)

[a] Crystal of $[(AgBF_4)\cdot\mathbf{1}]_n$ made from L- or D-peptide ligand **1**. [b] Number of molecules trapped in one pitch of channel A (based on the integral ratio of ligands **1** and **2** in the ^{1}H NMR spectrum). [c] Area ratio in chiral-phase HPLC traces.

from the Gly-D-Pro-D-Pro ligand (entry 2, Table 1). When a more highly concentrated solution (50 mM) of racemic **2** was used, about six molecules of **2** were trapped per helical pitch, but the enantiomeric selectivity was reduced (35% *ee*, entries 3,4, Table 1). The number of trapped molecules is almost saturated at this concentration as treating the crystal with a 100 mM solution of **2** (entries 5,6, Table 1) gave similar results. The observation of relatively high *ee* values is remarkable because guest **2** is considerably smaller than the nanosized channel.[11] Thus differentiation of the guest chirality presumably occurs on the interior surface of the nanosized peptidic helical channel.

Furthermore, large channel A is suited to the molecular recognition of large bio-oligomeric molecules. Maltopentaose **3**, a linear pentasaccharide composed of five D-glucose units (Glc) with $\alpha(1\rightarrow4)$ linkages, was successfully encapsulated within channel A. Guest encapsulation was carried out by simply soaking the single crystals in a methanol solution of **3** (20 mM) for one week at room temperature. After the crystals were separated from the mother liquor and decomposed by addition of aqueous NaCl, the filtrate was characterized by ^{1}H NMR spectroscopy. The molar ratio of ligand **1** and guest **3** was revealed to be approximately 10:1 by comparison of the integral ratio of the Glc H1 signals of **3** and Pro Hβ,γ signals of **1** (Supporting Information, Figure S24). Elemental analysis of the crystals also supported the encapsulation of **3** within the crystal at a ligand/guest ratio of around 10:1 (calcd. for $\{[(AgBF_4)\cdot\mathbf{1}]\cdot0.1(\mathbf{3})\cdot(H_2O)\cdot(CH_3OH)\}_n$: C 41.68, H 4.82, N 10.80%; found: C 41.52, H 4.99, N 10.91%). These data indicate that the space enclosed by two helical pitches of channel A was occupied by four to five molecules of **3**.[12] Figure 4 shows the geometry-optimized structure of **3** within channel A after a molecular dynamics simulation. However, encapsulation of **3** was unsuccessful when aqueous buffer (H_2O-MeOH = 1:1 (*v*/*v*) with 50 mM $NaBF_4$) was used as the solvent. This indicates that encapsulation of **3** within the crystals is enthalpically driven: presumably, **3** is efficiently trapped by hydrogen bonds between a number of hydroxy groups on **3** and amide carbonyl moieties on peptide **1** along

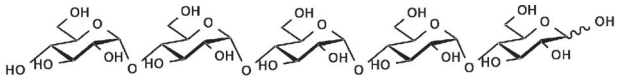

3

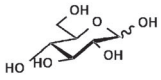

4

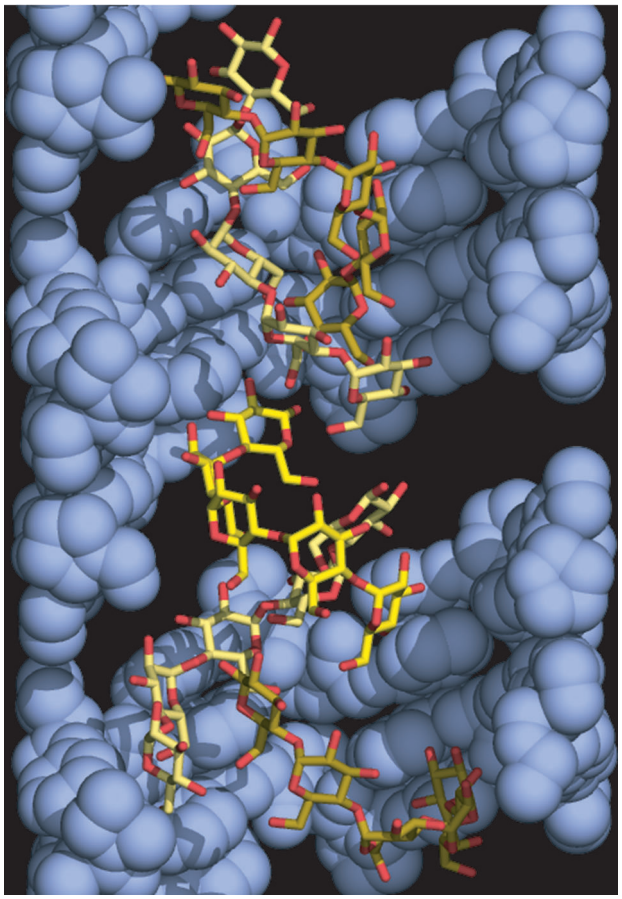

Figure 4. Geometry-optimized structure of **3** within large channel A of $[(AgBF_4)\cdot\mathbf{1}]_n$. Five molecules of **3** (yellow) in the space enclosed by two helical pitches of the duplex-like channel (24 ligands of **1**) are shown. The light blue space-filling representation shows the channel wall. Part of the channel wall is omitted for clarity.

the surface of channel A. Likewise, the encapsulation of D-glucose **4** failed in aqueous methanol but was successful in pure methanol. In this case, the space enclosed by two helical pitches of channel A was occupied by only approximately two molecules of **4**. These results also support the theory that maltopentaose **3** was efficiently trapped through the formation of multiple hydrogen bonds with the peptide helices on the channel framework. Thus, it was revealed that the channel with a diameter of 2 nm in the peptide-based crystalline material $[(AgBF_4)\cdot\mathbf{1}]_n$ is capable of molecular recognition of bio-oligomers.

In conclusion, we have created a new crystalline peptide-based porous material through coordination-driven self-assembly. A new strategy, namely a concerted processes of folding and networking, enabled us to construct a single crystalline nanoassembly of a short flexible peptide. Moreover, the folded peptidic helical conformation and unique entanglement provides 2 nm sized channels, which effectively recognize anions, organic chiral molecules, and bio-oligomers. We believe that in the future, such an artificial protein-like cavity will be applicable to the structural elucidation of bio-oligomers or their interactions.

Experimental Section

Preparation of a single crystal of $[(AgBF_4)\cdot1]_n$:

An aqueous solution of $AgBF_4$ (4.9 mg, 25 μmol, 150 μL), buffer solution (H_2O/EtOH = 1:1 (*v*/*v*), 150 μL), and an ethanolic solution of **1** (11.3 mg, 25 μmol, 150 μL) were triple-layered in a capped-microtube ($\phi = 6$ mm) and kept in a 10 °C incubator. After one week, a colorless block crystal ($320\times250\times250$ μm^3) was formed, and characterized by single crystal X-ray analysis. The crystals in three batches of microtubes were collected by filtration, and dried in vacuo (ca. 1 Torr) for 2 h at room temperature to give a crystalline powder 20.3 mg (yield 38%). Elemental analysis: calcd. for $\{[(AgBF_4)\cdot(\mathbf{1})]\cdot2.5(H_2O)\cdot0.5(C_2H_5OH)\}_n$: C 40.42, H 4.80, N 11.78%; found: C 40.25, H 4.77, N 11.85%.

Crystal data for $[(AgBF_4)\cdot\mathbf{1}]_n$: Hexagonal space group $P6_522$, $T = 90(2)$ K, $a = b = 37.4082(12)$, $c = 22.7505(15)$ Å, $V = 27571(2)$ Å^3, $Z = 12$, $\rho_{calcd} = 1.055$ Mg m^{-3}, $F(000) = 8982$, reflections collected/unique 236461/13512 ($R_{int} = 0.0587$). The structure was solved by direct methods (SHELXS-97) and refined by full-matrix least-squares methods (SHELXL-97) on F^2 with 771 parameters. $R_1 = 0.0794$ ($I > 2\sigma(I)$), $\omega R_2 = 0.2202$. GOF 1.181, CCDC 991706 contains the supplementary crystallographic data for this paper. These data can be obtained free of charge from The Cambridge Crystallographic Data Centre via www.ccdc.cam.ac.uk/data_request/cif.

Anion exchange experiments:

PF_6^-: Single crystals were picked up using a glass capillary, and put into an ethanol solution of $NaPF_6$ (50 mM, 450 μL) in a small vial. The vial was capped, and then incubated for 2 d at 10 °C. X-ray analyses were then carried out. Crystal data for $[(AgPF_6)\cdot\mathbf{1}]_n$: Hexagonal space group $P6_522$, $T = 90(2)$ K, $a = b = 37.2943(17)$, $c = 23.893(2)$ Å, $V = 28779(3)$ Å^3, $Z = 12$, $\rho_{calcd} = 1.024$ Mg m^{-3}, $F(000) = 9042$, reflections collected/unique 138402/6784 ($R_{int} = 0.0557$). 758 parameters. $R_1 = 0.1024$ ($I > 2\sigma(I)$), $\omega R_2 = 0.2935$. GOF 0.915, CCDC 991707.

$CF_3SO_3^-$: Single crystals were put into an ethanol solution of NaOTf (100 mM, 450 μL) and incubated for three weeks at 10 °C. Crystal data for $[(AgCF_3SO_3)\cdot\mathbf{1}]_n$: Hexagonal space group $P6_522$, $T = 90(2)$ K, $a = b = 37.693(2)$, $c = 23.893(3)$ Å, $V = 29398(4)$ Å^3, $Z = 12$, $\rho_{calcd} = 0.982$ Mg m^{-3}, $F(000) = 8874$, reflections collected/unique 162519/8383 ($R_{int} = 0.0499$). 762 parameters. $R_1 = 0.0977$ ($I > 2\sigma(I)$), $\omega R_2 = 0.2806$. GOF 0.831, CCDC 991708.

Chiral recognition of 1,1′-bi-2-naphthol (**2**): Several single crystals were picked up using a glass capillary, and put into an ethanol solution of racemic **2** (10 mM, 450 μL) in a small vial. The vial was capped, and then incubated at 10 °C. After two weeks, the mother liquor was removed, washed with fresh ethanol (four times), and the crystals were dried under reduced pressure. The dried crystals were decomposed by the addition of 50 mM aq. NaCl (ca. 0.5 mL) and the mixture was lyophilized. $CDCl_3$ was added to the resulting solid, and the solution was analyzed by ^{1}H NMR spectroscopy to estimate the uptake of guest molecules within the crystals. The NMR sample was then washed with 1N aq. HCl to remove peptide-containing ligand **1**. The organic layer was dried over Na_2SO_4, and the supernatant was concentrated and injected into an analytical HPLC (DAICEL CHIRALPAK IA column, eluent: $CHCl_3$) to analyze the enantiomeric ratio of encapsulated **2**.

Encapsulation of maltopentaose (**3**): Several single crystals were picked up using a glass capillary, and put into a methanol solution of maltopentaose (20 mM, 450 μL) in a small vial. The vial was capped, and then incubated for one week at room temperature.

Elemental analysis: After being separated from the mother liquor, the crystals were washed with a small amount of methanol (four times) and dried in vacuo (ca. 1 Torr) for 24 h at 55 °C.

NMR analysis: After being separated from the mother liquor, the crystals were washed with a small amount of methanol (four times). The dried crystals were decomposed by addition of 50 mM aq. NaCl (ca. 0.5 mL). After the precipitated AgCl was removed by filtration, the filtrate was lyophilized overnight. The obtained solid was dissolved in D_2O and characterized by ^1H NMR spectroscopy (Supporting Information, Figure S23).

Molecular modeling: Five molecules of **3** were placed at the void of two helical pitches of the duplex-like channel of $[(AgBF_4)\cdot\mathbf{1}]_n$, and structural annealing was conducted from 1000 K to 300 K by a molecular dynamics (MD) simulation. Solvents were excluded in this calculation. Geometry optimization was then applied to one of the energy minimized structures. The Universal force field was used, and the coordinates of the channel framework were kept rigid during the geometry optimization. Materials Studio 6.0 (Accelrys) was used for this calculation.

Received: March 20, 2014
Revised: May 1, 2014
Published online: May 23, 2014

Keywords: chiral recognition · coordination · molecular recognition · peptide folding · self-assembly

[1] A. V. Kajava, *J. Struct. Biol.* **2012**, *179*, 279 – 288.
[2] a) M. Fujita, M. Tominaga, A. Hori, B. Therrien, *Acc. Chem. Res.* **2005**, *38*, 371 – 380; b) Y. Takezawa, M. Shionoya, *Acc. Chem. Res.* **2012**, *45*, 2066 – 2076; c) T. R. Cook, Y.-R. Zheng, P. J. Stang, *Chem. Rev.* **2013**, *113*, 734 – 777; d) M. M. J. Smulders, I. A. Riddell, C. Browne, J. R. Nitschke, *Chem. Soc. Rev.* **2013**, *42*, 1728 – 1754; e) K. Harris, D. Fujita, M. Fujita, *Chem. Commun.* **2013**, *49*, 6703 – 6712.
[3] a) O. M. Yaghi, M. O'Keeffe, N. W. Ockwig, H. K. Chae, M. Eddaoudi, J. Kim, *Nature* **2003**, *423*, 705 – 714; b) S. Kitagawa, R. Kitaura, S. Noro, *Angew. Chem. Int. Ed.* **2004**, *43*, 2334 – 2375; *Angew. Chem.* **2004**, *116*, 2388 – 2430; c) G. Férey, C. Mellot-Draznieks, C. Serre, F. Millange, *Acc. Chem. Res.* **2005**, *38*, 217 – 225; d) L. Ma, C. Abney, W. Lin, *Chem. Soc. Rev.* **2009**, *38*, 1248 – 1256; e) Y. Inokuma, M. Kawano, M. Fujita, *Nat. Chem.* **2011**, *3*, 349 – 358.
[4] For this reason, many reports have resulted in soft materials such as gels, fibers, and nanoparticles: A. M. Kushner, Z. Guan, *Angew. Chem. Int. Ed.* **2011**, *50*, 9026 – 9057; *Angew. Chem.* **2011**, *123*, 9190 – 9223.
[5] In the field of peptide chemistry, precise peptide assemblies have been approached by using cyclic peptides or de novo designed coils: a) M. R. Ghadiri, J. R. Granja, R. A. Milligan, D. E. McRee, N. Khazanovich, *Nature* **1993**, *366*, 324 – 327; b) Y. Lim, K.-S. Moon, M. Lee, *Angew. Chem. Int. Ed.* **2009**, *48*, 1601 – 1605; *Angew. Chem.* **2009**, *121*, 1629 – 1633; c) K. Matsuura, K. Watanabe, T. Matsuzaki, K. Sakurai, N. Kimizuka, *Angew. Chem. Int. Ed.* **2010**, *49*, 9662 – 9665; *Angew. Chem.* **2010**, *122*, 9856 – 9859; d) G. Grigoryan, Y. H. Kim, R. Acharya, K. Axelrod, R. M. Jain, L. Willis, M. Drndic, J. M. Kikkawa, W. F. DeGrado, *Science* **2011**, *332*, 1071 – 1076; e) J. M. Fletcher, R. L. Harniman, F. R. H. Barnes, A. L. Boyle, A. Collins, J. Mantell, T. H. Sharp, M. Antognozzi, P. J. Booth, N. Linden, M. J. Miles, R. B. Sessions, P. Verkade, D. N. Woolfson, *Science* **2013**, *340*, 595 – 599.
[6] a) See the following review articles and references therein about metal – biomolecule frameworks: I. Imaz, M. Rubio-Martínez, J. An, I. Solé-Font, N. L. Rosi, D. Maspoch, *Chem. Commun.* **2011**, *47*, 7287 – 7302; b) a pentapeptide has been incorporated in a metal-peptide crystal; however, metal cross-linking has been observed between three residues length at the longest to date: D. Peri, J. Ciston, F. Gándara, Y. Zhao, O. M. Yaghi, *Inorg. Chem.* **2013**, *52*, 13818 – 13820; c) cooperative folding behavior after the formation of crystalline zinc-dipeptide β-sheets has been reported very recently: C. Martí-Gastaldo, D. Antypov, J. E. Warren, M. E. Briggs, P. A. Chater, P. V. Wiper, G. J. Miller, Y. Z. Khimyak, G. R. Darling, N. G. Berry, M. J. Rosseinsky, *Nat. Chem.* **2014**, *6*, 343 – 351.
[7] In the case of fully folded proteins, the creation of crystalline materials by metal linkages has been reported recently: J. D. Brodin, X. I. Ambroggio, C. Tang, K. N. Parent, T. S. Baker, F. A. Tezcan, *Nat. Chem.* **2012**, *4*, 375 – 382.
[8] See the Supporting Informationfor details.
[9] G. A. Petsko, D. Ringe, *Protein Structure and Function*, New Science Press, London, **2004**.
[10] The hexagonal entanglements are illustrated in the Supporting Information, Figure S14.
[11] The pore size effect on enantioselective separation by homochiral metal – organic frameworks has been discussed: Y. Liu, W. Xuan, Y. Cui, *Adv. Mater.* **2010**, *22*, 4112 – 4135.
[12] In the crystalline network $[(AgBF_4)\cdot\mathbf{1}]_n$, 50% of ligand **1** forms channel A and the remaining 50% forms channel B.

